Materials Research Express

INCLUSIVE PUBLISHING TRUSTED SCIENCE
PURPOSE-LED PUBLISHING™

PAPER • **OPEN ACCESS**

Evaluation of microstructure and mechanical behavior of Ti_p/AZ91 composites produced by hot press sintering

To cite this article: Fevzi Kelen 2026 *Mater. Res. Express* **13** 216506

View the article online for updates and enhancements.

You may also like

- Study of burning rate characteristics of propellants containing Al–Mg alloy nanopowder
Mohammed Iqbal C, Santhosh Kumar L, S R Chakravarthy et al.
- Effects of SiC contents on mechanical properties and thermal conductivity of SiC/Mg composites
Jianbo Nie, Lingling Fan, Xianwen Lu et al.
- Angled etching of Si by ClF_3–Ar gas cluster injection
Toshio Seki, Hiroki Yamamoto, Takahiro Kozawa et al.

This content was downloaded from IP address 193.255.143.78 on 16/11/2026 at 05:54

Materials Research Express

Check for updates

OPEN ACCESS

RECEIVED
29 July 2026

REVISED
27 September 2026

ACCEPTED FOR PUBLICATION
3 November 2026

PUBLISHED
10 November 2026

Original content from this work may be used under the terms of the Creative Commons Attribution 4.0 licence.

Any further distribution of this work must maintain attribution to the author(s) and the title of the work, journal citation and DOI.

PAPER

Evaluation of microstructure and mechanical behavior of Ti_p/AZ91 composites produced by hot press sintering

Fevzi Kelen*

Automotive Program, Department of Motor Vehicles and Transport Technology, Van Vocational High School, Van Yuzuncu Yil University, Van 65080, Türkiye

* Author to whom any correspondence should be addressed.

E-mail: fkelen@yyu.edu.tr

Keywords: AZ91, Ti, composites, hot press sintering, automotive materials

Abstract

In the present study, the density, morphological characteristic and mechanical properties at both room and elevated temperatures of titanium microparticle-reinforced AZ91 matrix composites were evaluated. Density measurements of the specimens indicated a close agreement between the theoretical and experimental values. Porosity was determined to be below 1% in all specimens. Morphological analyses revealed that the titanium particles were located along the grain boundaries of the matrix alloy and exhibited a relatively uniform distribution. The field emission scanning electron microscopy, energy-dispersive x-ray spectroscopy, and x-ray diffraction analyses identified the presence of α-Mg, β-$Mg_{17}Al_{12}$, and Ti phases. No additional phases were detected beyond these. In this context, a pore-free microstructure devoid of secondary phases was obtained at the matrix–reinforcement interface. Compression tests revealed that both the yield and compressive strengths, as well as the ductility, were significantly improved compared to the monolithic alloy. At room temperature, the composites exhibited maximum values of 213.9 MPa for yield strength, 464.9 MPa for compressive strength, and 18.5% for ductility. These values show increases of approximately 18%, 90.5%, and 68%, respectively, compared to the monolithic alloy. Furthermore, a similar trend was observed at elevated temperatures, where the corresponding values remained significantly higher than those of the monolithic alloy. Due to their low density and superior mechanical properties at both room and elevated temperatures, composite specimens constitute a viable option for industrial applications, including the automotive sector.

1. Introduction

In transportation applications such as automotive and aerospace, structural weight poses a significant challenge in terms of energy consumption. Furthermore, internal combustion engines, commonly referred to as conventional engines, contribute to a significant increase in exhaust emissions. On the other hand, it leads to critical driving and handling issues, such as poor maneuverability, low acceleration, and weak braking performance. The mitigation of all these drawbacks is achievable only through the reduction of structural weight [1, 2]. Among engineering materials, magnesium and its alloys stand out due to their low density. Among these, the AZ91 alloy series is widely used in industry compared to others. However, its usage remains below the desired level compared to that of iron and steel, as well as aluminum and its alloys. The main reason for this is the insufficient inherent properties under service conditions [3, 4]. In alloying and composite studies aimed at overcoming the disadvantages of the AZ91 series, high-performance materials generally exhibit high costs, while others face significant issues such as insufficient ductility, low strength, or inadequate performance in both properties. In this context, research and development efforts are still ongoing. In the literature, the majority of experimental approaches have focused on composites. In composite processing, the aim is to simultaneously enhance mechanical characteristics such as both strength and ductility [5, 6]. In selecting reinforcement elements based on the mechanical and physical properties of the master alloy, metal-based reinforcements have

© 2026 The Author(s). Published by IOP Publishing Ltd

emerged as the preferred choice. These reinforcements, in particular, offer a critical advantage in their application due to exhibiting similar characteristics. In experiments where copper [7, 8], nickel [9, 10], titanium [11–20], and their alloys [21–25], or combinations thereof [26, 27], were used as reinforcement elements, titanium-based reinforcements have shown great potential due to their identical crystal structure with the master alloy and relatively low density compared to the others [28, 29]. In titanium-reinforced magnesium matrix composites, the hexagonal crystal structure of the reinforcement at room temperature facilitates strong interfacial bonding, leading to improvements not only in yield strength, tensile strength, elastic modulus, and compressive resistance but also in fracture strain. Moreover, by inducing a grain-refining effect in the microstructure, it has significantly contributed to the enhancement of strength (Orowan mechanism). In solid-state production processes, it has been reported that, in addition, no chemical reactions occur between the matrix and the reinforcement, and no undesirable hard and brittle secondary phases are formed. This is because hard and brittle secondary phases negatively affect the material's ability to undergo plastic deformation under load, leading to reduced strength. Furthermore, morphological analyses of these composites have shown that porosity is either minimal or within acceptable levels [30–40]. However, in none of these studies was a high content of reinforcement employed. Moreover, the mechanical properties of the composite materials, such as high-temperature yield strength, compressive strength, and fracture strain, have not been systematically investigated.

In the current approach, four different compositions of composite materials produced using the hot-press sintering technique were investigated. Initially, the matrix alloy was reinforced with a low content of reinforcement, after which the reinforcement fraction was increased to higher levels. The effect of titanium content on the microstructural characteristics of the matrix alloy, as well as on the room- and high-temperature yield strength, compressive strength, and fracture strain of the composite materials, was studied. Additionally, in the solid-state production, the morphological and mechanical characteristics of unreinforced and reinforced specimens were compared to establish a systematic approach.

2. Experimental procedure

2.1. Materials and fabrication

AZ91 alloy particles from the starting powders were used as the matrix, while titanium particles served as the reinforcement material. The matrix and reinforcement powders were purchased from TangShan WeiHao Magnesium Powder Co., Ltd (China) and Alfa Aesar (Germany), respectively. The powders had a purity of 99%, and their chemical compositions are presented in table 1. While the titanium particles had an average size of 45 μm, the matrix alloy particles ranged approximately three to six times larger. For composite production, the powders were mechanically mixed in a ceramic container using a spatula for approximately 10 min at volume fractions of 0%, 10%, 20%, and 30%, and then placed into cylindrical graphite molds with an inner diameter of 40 mm for hot-press sintering. Subsequently, based on the Mg–Al binary phase diagram [41], the production parameters were optimized to a temperature of 420 °C, a pressure of 50 MPa, and a holding time of 1 h. The solid-state sintering process was carried out entirely under an argon atmosphere, and after the apparatus cooled to room temperature, the specimens were removed from the molds. After material fabrication, all specimens were cut to dimensions of $5 \times 5 \times 10$ mm^3 using wire electrical discharge machining and prepared for density measurements, morphological analysis, and mechanical testing.

2.2. Density measurements

The theoretical densities of the composite materials were calculated using Archimedes' principle [42]. The experimental densities of the reference and composite samples were determined using four randomly selected specimens from each, which had previously undergone metallographic preparation. In the experimental studies, distilled water was used as the fluid, and an analytical balance with a sensitivity of 0.0001 g was employed. The specimens were first measured in air and then fully immersed in the liquid for the measurements. The following equations were used, in order, to calculate the theoretical density, experimental density, and porosity values,

$$\rho_{th} = V_r \rho_r + (1 - V_r)\, \rho_m \tag{1}$$

$$\rho_e = \frac{W_a . \rho_w}{W_a - W_w} \tag{2}$$

$$P = 1 - \frac{\rho_e}{\rho_{th}} \times 100. \tag{3}$$

Table 1. Chemical composition of the starting powders.

	Element content, wt.%									
Materials	Al	Zn	Mn	Cu	Fe	Be	Ni	Si	Mg	Ti
AZ91	8.93	0.4294	0.19	0.0008	0.010	0.0010	0.003	0.029	90.40	—
Ti	—	—	—	—	—	—	—	—	—	Balan.

Here, ρ_{th}, ρ_r, ρ_m, V_r, ρ_e, W_a, ρ_w, W_w, and P represent the theoretical density of the specimen, the density of the reinforcement material, the density of the matrix, the volume fraction of the reinforcement, the experimental density of the specimen, the weight of the specimen in air, the density of water, the weight of the specimen in water, and the porosity of the specimen, respectively [43].

2.3. Microstructure observations

Field emission scanning electron microscopy (FESEM), EDX (energy-dispersive x-ray spectroscopy), and x-ray diffraction (XRD) analyses were performed using Zeiss Sigma 300 and PANalytical Empyrean instruments, respectively. The interaction of the reinforcement phase with the matrix and its distribution characteristics in the microstructure were examined using FESEM, the elemental composition trends of the sintered materials were analyzed by energy dispersive x-ray spectroscopy, and the phase composition behavior of the specimens was investigated using XRD. Prior to morphological examinations, all specimens underwent metallographic preparation, with their surfaces polished and etched. For polishing, the surfaces of the specimens, previously cleaned with 240–1200 grit sandpapers, were treated using diamond suspensions of 1–3 μm, while a solution of 5 vol.% nitric acid (HNO_3) and 95 vol.% ethanol (CH_3CH_2OH) was used as the etchant.

2.4. Mechanical characterization

The mechanical properties, including yield strength, compressive strength, and fracture strain, of unreinforced and reinforced specimens produced via uniaxial hot-press sintering were determined through compressive tests conducted at four different temperatures. Although studies on the room-temperature mechanical behavior of titanium-reinforced matrix alloys exist in the literature, information regarding their load-bearing performance at elevated temperatures is scarce. In this context, the mechanical behavior of the produced specimens at both room and elevated temperatures was systematically characterized and presented. Furthermore, the plastic deformation capacities of the composite materials at room temperature as well as at 150 °C, 175 °C, and 200 °C were determined to assess their suitability for automotive service conditions [44]. In the mechanical tests, an electromechanical universal compression testing machine with a test speed of 0.2 mm min^{-1} was used.

3. Results and discussion

3.1. Density and porosity

The theoretical density, experimental density, and porosity of the monolithic matrix alloy and composite materials containing titanium particles at different volume fractions are presented in table 2. It was observed that the difference between the theoretical and experimental densities in both the unreinforced matrix alloy and the reinforced specimens was minimal. The monolithic alloy nearly reached full density. In the composites, the density increased with the reinforcement content, reaching 2.598 g cm^{-3} in the specimen with the highest reinforcement fraction. A similar trend was observed in the porosity of the composite materials. In the specimen containing the lowest amount of titanium, porosity was 0.336%, whereas it increased to 0.726% in the sample with the highest reinforcement content. However, in both the unreinforced matrix alloy and all composite materials, porosity remained below 1% due to effective pressing and sintering. Furthermore, even at the highest titanium content, the density of the composite materials remained well below that of aluminum and its alloys [45].

3.2. Microstructure

FESEM images of the composite materials are presented in figure 1. These analyses show that, following hot pressing, there was no significant grain growth in the matrix alloy. In the base material, although this is largely attributed to effective pressing and sintering, the grain-refining effect of the reinforcement material also plays a role [26, 27, 46, 47]. This is because titanium has been reported in the literature to possess a grain-refining effect. Morphological examinations revealed that the reinforcement phase

Table 2. Theoretical density, experimental density, and porosity of the monolithic matrix alloy and composites.

Serial no	Materials	Theoretical density (g cm^{-3})	Experimental density (g cm^{-3})	Relative density (%)	Porosity (%)
1	AZ91 alloy	1.81	1.805 ± 0.01	0.99724	0.276 ± 0.01
2	AZ91-10%Ti_p	2.079	2.072 ± 0.01	0.99663	0.336 ± 0.02
3	AZ91-20%Ti_p	2.348	2.336 ± 0.02	0.99489	0.511 ± 0.02
4	AZ91-30%Ti_p	2.617	2.598 ± 0.01	0.99274	0.726 ± 0.02

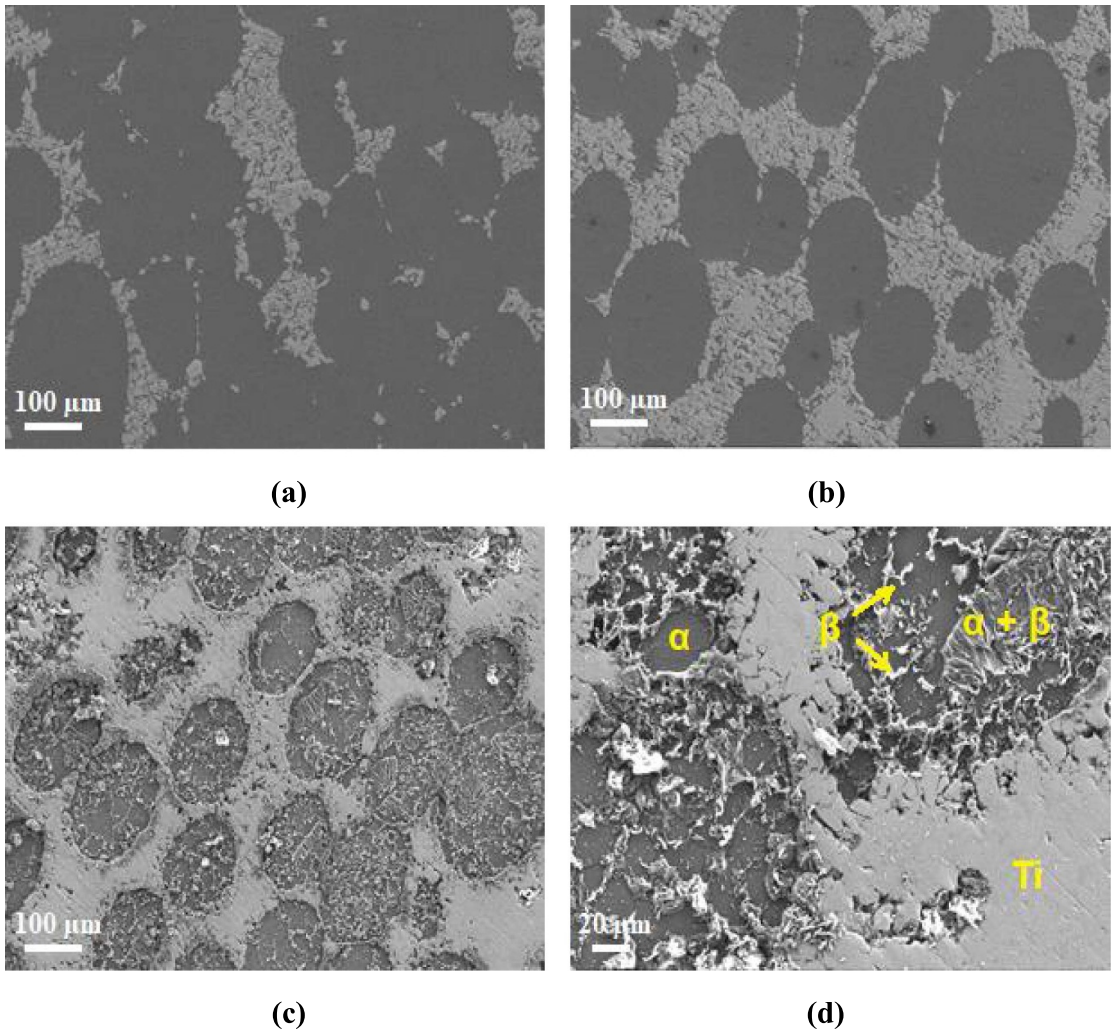


Figure 1. FESEM analyses of the composite materials: (a) AZ91-10%Ti_p, (b) AZ91-20%Ti_p, (c) and (d) AZ91-30%Ti_p.

was located along the grain boundaries of the matrix alloy, forming a pore-free interface. These images clearly indicate that both the matrix alloy and the reinforcement powders were well-sintered with each other at the processing temperature. The very low porosity observed in the microstructure was found to occur primarily between the reinforcement particles (figure 1(d)). This is attributed to the higher melting temperature of the reinforcement powders compared with that of the matrix alloy [48], the difference in particle size between the powders, and the applied pressure. As revealed by etching to expose the internal structure and as can be seen from the FESEM image of the specimen with the highest reinforcement at high magnification (figure 1(d)), the composite materials consist of α-Mg, β-$Mg_{17}Al_{12}$, and Ti phases. This is because, at the processing temperature of the composites, it is evident that no chemical reactions occur between the matrix alloy and the reinforcement phase in the Mg–Ti [49], Al–Ti [50], and Zn–Ti [51] systems. In this context, a clean, well-bonded, and pore-free interface, devoid of secondary phases, was achieved in the composite materials.

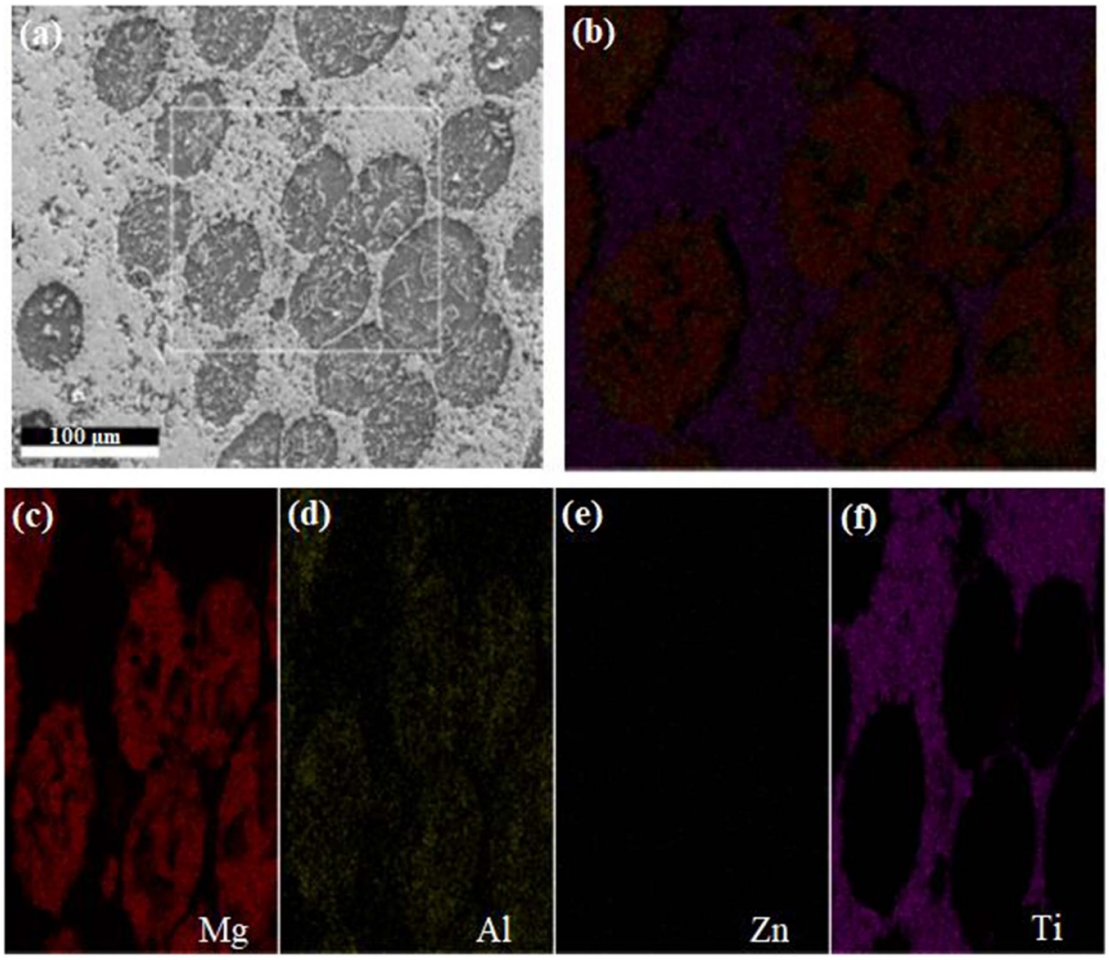


Figure 2. X-ray elemental analysis of the AZ91-30%Ti_p specimen: (a) mapping area, (b) elemental distribution, (c) Mg, (d) Al, (e) Zn, and (f) Ti elements.

Figure 2 presents the x-ray elemental mapping analysis of the composite material containing the maximum amount of titanium. In these analyses, magnesium, aluminum, zinc, and titanium elements were selected for mapping. The EDX analysis shows the distribution of the existing phases within the structure. While only Mg, Al, and Zn phases are present in the matrix alloy, the reinforcement region contains the titanium phase. It was observed that the concentrations of these phases drop to zero at the interface. No phases other than Mg, Al, Zn, and Ti were detected in the elemental mapping. As explained above, this is due both to the absence of any secondary phase formation at the matrix–reinforcement interface during the processing of the composite materials and to the use of a protective inert atmosphere throughout all stages of material fabrication. Moreover, the absence of contaminants such as oxygen, carbon, and nitrogen in the analyses indicates that the fabrication process was successfully carried out. The phases identified in the FESEM analyses corresponded to those detected in the EDX elemental mapping, and no additional phases were observed in either type of analysis. Therefore, the FESEM and EDX analyses are consistent with each other as well as with the literature [26, 27, 52, 53].

The XRD patterns of the monolithic matrix alloy and composites containing titanium in different volume fractions are presented in figure 3. The matrix alloy retains the same phases as the initial powders after hot pressing, which correspond exactly to the standard peaks of α-Mg (JCPDS 04-0770) and β-$Mg_{17}Al_{12}$ (JCPDS 73-1148). In addition to these phases, the composite samples also contain the titanium phase (α-Ti). The peaks of the reinforcing phase coincide exactly with the standard peaks of the hexagonal α-Ti phase (JCPDS 44-1294), and they become more pronounced with increasing titanium content. The $\alpha'(100)$ and $\alpha'(101)$ peaks of titanium, located between 2θ: 34° and 2θ:41°, were masked by the corresponding magnesium peaks at 2θ:34.981° and 2θ: 40.012°, respectively. In contrast, the $\alpha'(002)$ peak of the reinforcement phase at 2θ:38.211° is clearly observed in the specimen containing the maximum reinforcement content, and its intensity increases with increasing titanium content.

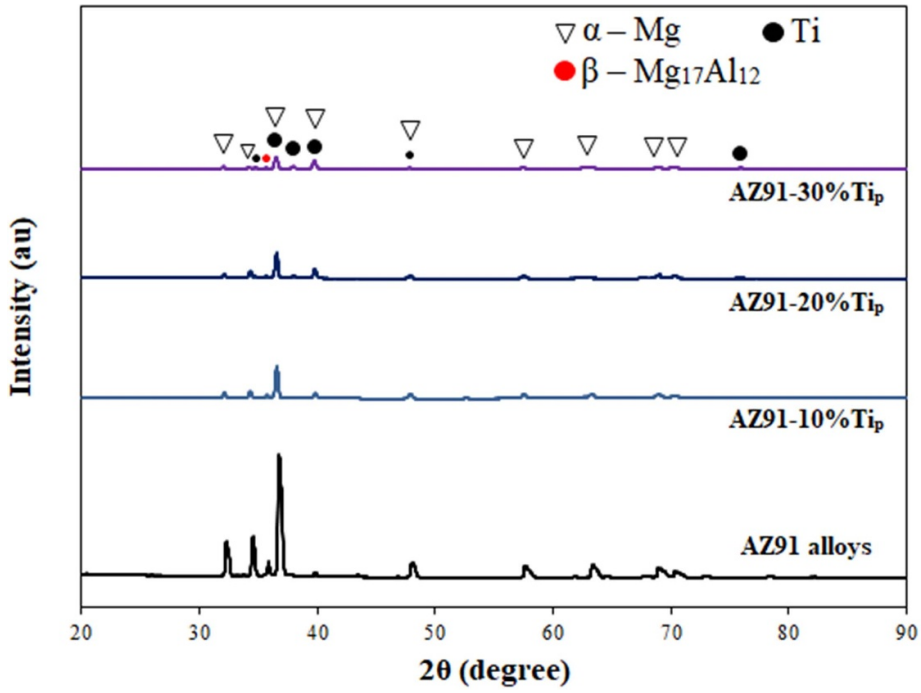


Figure 3. XRD patterns of the monolithic alloy and composites.

On the other hand, a similar trend was observed for the $\alpha'(110)$ peak of the reinforcement phase at 2θ:63.605°. Similar to the other peaks, this peak was also masked by the magnesium peak at 2θ:63.542°. However, the XRD pattern exhibited these peaks as a single broad peak rather than as distinct individual peaks. Additionally, the $\alpha'(103)$ peak of titanium at 2θ:70.906° also overlaps with the magnesium peak at 2θ:70.554°. As the reinforcement content increased, the intensity of the magnesium peak decreased, whereas the opposite trend was observed for the titanium peak. Moreover, the $\alpha'(112)$ and $\alpha'(201)$ peaks of the reinforcement at 2θ:75.738° and 2θ:76.263° are detected as a single peak rather than separately by XRD. The standard peaks of the reinforcing phase can be almost entirely observed in the sample with the highest reinforcement content. The phases identified in FESEM and EDX analyses were also detected in the XRD analysis. In this context, the microstructural analyses corroborate each other.

3.3. Mechanical properties

Considering the ASTM E 9-89a [54] standard, the graphs of yield strength, compressive strength, and fracture strain from mechanical compression tests conducted at different temperatures are presented in figure 4. It was observed that, under room-temperature stress, the matrix-alloy composites with dimensions of 5 × 5 × 10 mm^3 exhibited significant increases in yield strength, compressive strength, and fracture strain compared to the unreinforced sample, indicating the strengthening effect of the reinforcement phase. The mechanical properties reached their highest values, particularly at a reinforcement content of 20%. However, although further additions beyond this point still show an increase compared to the matrix alloy, a decrease is observed relative to the other composite types. While the room-temperature yield strength, compressive strength, and fracture strain of the unreinforced sample were 181.2 MPa, 244 MPa, and 11.00%, respectively, the addition of 20 vol.% titanium to the matrix alloy increased these values to 213.9 MPa, 464.9 MPa, and 18.5%, respectively. These correspond to significant increases of approximately 18% in yield strength, 90.5% in compressive strength, and 68% in fracture strain. As mentioned above, further additions beyond this level still show an improvement compared to the monolithic matrix alloy, but a decrease is observed relative to the other two composite types. For example, the material containing 10 vol.% reinforcement exhibited a yield strength, compressive strength, and fracture strain of 198.6 MPa, 408.1 MPa, and 15.02%, respectively, whereas when the reinforcement content was increased to 30%, these values decreased to 185.3 MPa, 308.5 MPa, and 14.53%, respectively. In this type of sample, compared to the unreinforced matrix alloy, increases of approximately 2%, 26%, and 32% were observed in yield strength, compressive strength, and fracture strain, respectively. Therefore, the addition of titanium resulted in improvements in the yield strength, compressive strength, and fracture strain of the matrix alloy, even at the maximum reinforcement content. The increase in

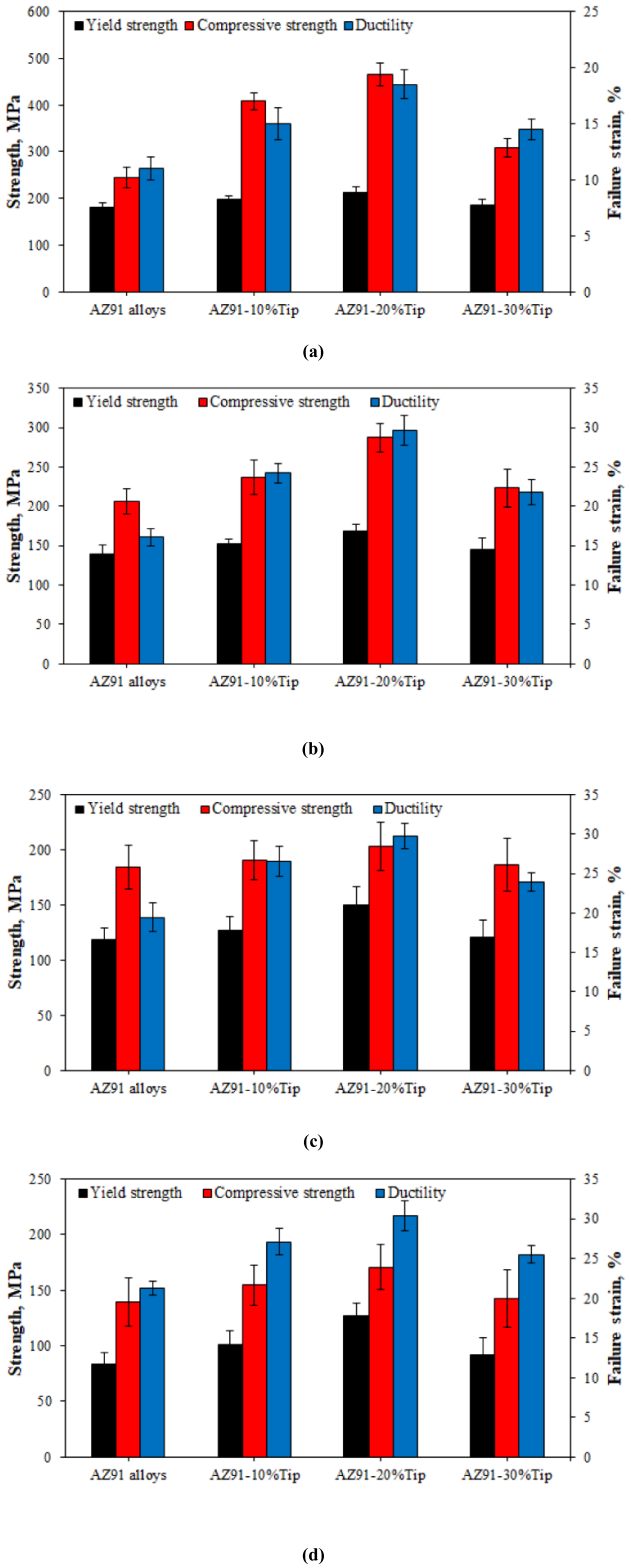


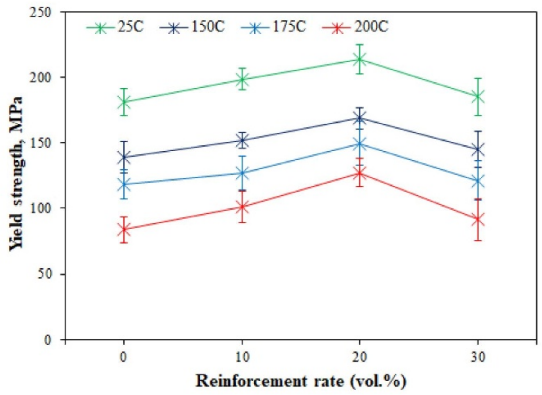
Figure 4. Graphs of yield strength, compressive strength, and fracture strain of the matrix alloy and composites at (a) room temperature, (b) 150 °C, (c) 175 °C, and (d) 200 °C, respectively.

fracture strain, in particular, is significant and noteworthy. This behavior is attributed to the optimized production parameters, the presence of the β phase, the matching room-temperature crystal structures of the matrix alloy and the reinforcement material, and the favorable properties of titanium, including high yield strength, high elastic modulus, and high melting temperature. This is because the softening of the β-$Mg_{17}Al_{12}$ intermetallic phase in the matrix alloy at the processing temperature ($\sim$120 °C and above [55]) enhances the pressing and sintering capabilities of the matrix particles, thereby strengthening

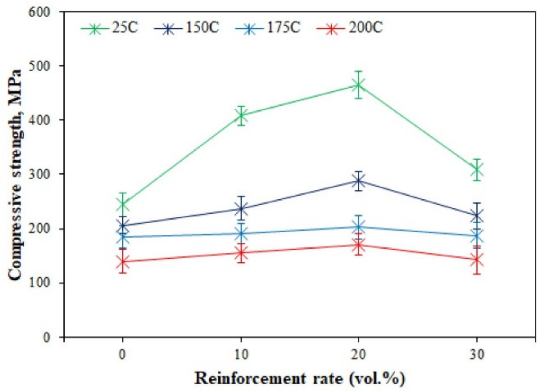
the matrix–reinforcement interaction. Thus, a sound and well-formed microstructure free of secondary phases and porosity was developed at the interface. Moreover, the room-temperature hexagonal crystal structures of the matrix alloy and titanium positively influence the interfacial properties. For these reasons, significant increases were observed in the compressive strength and fracture strain of the composite materials. These high values are particularly remarkable, with the maximum levels achieved at a reinforcement content of 20 vol.%. Furthermore, even at titanium contents above 20%, improvements were still observed compared to the monolithic matrix alloy. The current situation, which is quite rarely reported in the literature, demonstrates that the use of titanium as a reinforcement material is critical for overcoming the inherent limitations of the matrix alloy. This is because, in experimental studies aimed at eliminating the disadvantages of the matrix alloy, such an effect has not been observed with carbide, boride, nitride, or oxide reinforcements [56–59]. Although carbide-containing materials exhibit high mechanical properties such as strength and hardness, their fracture strain has been reported to be very low. A similar behavior was observed in boride, nitride, and oxide-reinforced materials, where the fracture strain was adversely affected. In the case of metal reinforcement elements, both strength and fracture strain were improved; however, it was observed that the fracture strain decreased with increasing reinforcement content [7, 8, 10, 25–27].

A similar behavior was observed in the mechanical compression tests of the composite materials conducted at 150 °C, 175 °C, and 200 °C, as compared to room temperature. As can be seen in figure 4(b), c, and d, the highest values among the three composite types were again obtained in the sample containing 20 vol.% titanium. This material exhibited superior yield strength, compressive strength, and fracture strain behavior compared to both the monolithic alloy and the other composites, at both room and elevated temperatures. The yield strengths of the AZ91-20%Ti_p sample were determined to be 168.9 MPa, 149.8 MPa, and 127.3 MPa at 150 °C, 175 °C, and 200 °C, respectively. Compared to the unreinforced matrix alloy, significant increases in yield strength of approximately 21%, 26.5%, and 52% were observed at the same temperatures, respectively. Moreover, in terms of compressive strength at the same temperatures, improvements of approximately 39%, 10%, and 22% were achieved compared to the monolithic alloy, respectively. At these temperatures, the fracture strain values were measured as 29.61%, 29.82%, and 30.41%, respectively. Significant increases in fracture strain were also observed compared to the monolithic alloy. This is because, at the same temperatures, the fracture strain values of the monolithic alloy were determined to be 16.05%, 19.44%, and 21.03%, respectively. Among the other composite materials, the yield strength, compressive strength, and ductility of the AZ91-10%Ti_p sample were determined as 152.2 MPa, 236.8 MPa, and 24.2%; 127.1 MPa, 190.9 MPa, and 26.6%; and 101.4 MPa, 154.8 MPa, and 27.12% at 150 °C, 175 °C, and 200 °C, respectively. The mechanical properties, including yield strength, compressive strength, and fracture strain, obtained from mechanical compression tests conducted at room temperature as well as at 150 °C, 175 °C, and 200 °C on titanium-reinforced AZ91 magnesium matrix composites produced via uniaxial hot pressing, were found to be higher compared to the monolithic alloy. The relatively lower mechanical properties observed in the composites at maximum reinforcement content, compared to the AZ91-10%Ti_p and AZ91-20%Ti_p samples, are attributed to the high reinforcement fraction. This is because, at the maximum reinforcement level, the increased amount of titanium weakened the interactions both among the titanium particles themselves and between the particles and the matrix alloy. Although the β-$Mg_{17}Al_{12}$ intermetallic phase in the matrix alloy softens at the processing temperature, facilitating effective pressing and sintering, this effect was not sufficient to fully counteract the issue. Moreover, the presence of titanium particles at the grain boundaries of the matrix alloy has contributed positively to the strength. As can also be seen from the FESEM images shown in figure 1, the placement of the reinforcement powders at the grain boundaries of the matrix alloy, which inhibits grain growth (i.e. the grain-refining effect), contributed to limiting the reduction in yield strength, compressive strength, and ductility. This is further confirmed by the fact that, as noted above, even at the maximum titanium content, the mechanical properties remain superior to those of the monolithic alloy. Moreover, it is particularly noteworthy that even at the maximum titanium content, the fracture strain remains higher than that of the unreinforced matrix alloy.

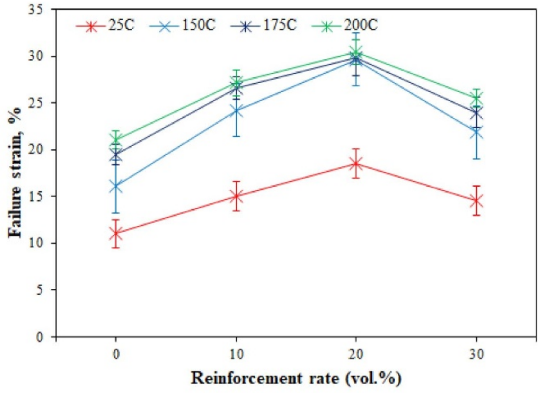
The effect of titanium addition to the matrix alloy on yield strength, compressive strength, and fracture strain at room temperature as well as at 150 °C, 175 °C, and 200 °C is presented in figure 5. In the composite samples, the highest yield strength and compressive strength values were obtained at room temperature, whereas, as expected, the highest fracture strain values were observed at 200 °C. The addition of titanium resulted in a linear increase in yield strength of the composite materials up to a reinforcement content of 20 vol.% (figure 5(a), green line). Beyond this level, the yield strength was adversely affected, resulting in a decrease. A similar trend was observed at 150 °C, 175 °C, and 200 °C,



(a)



(b)



(c)

Figure 5. Effect of titanium content on the mechanical properties of the composite materials: (a) yield strength, (b) compressive strength, (c) fracture strain.

as at room temperature. However, the slope of the decrease at 200 °C (figure 5(a), red line) is relatively steeper compared to the others. The primary reason for this is the β-$Mg_{17}Al_{12}$ intermetallic phase present in the matrix alloy. This intermetallic compound softens more at the test temperature of 200 °C, leading to a more rapid decrease in yield strength compared to the values at 150 °C and 175 °C. In terms of compressive strength, the highest values were again achieved at room temperature with a reinforcement content of 20 vol.% (figure 5(b), green line). Beyond this reinforcement level, a decrease was observed at all test temperatures, similar to the trend seen in yield strength. However, unlike yield strength, the steepest decline in compressive strength was observed at room temperature (figure 5(b), green line). This behavior, as explained above, is attributed to the high reinforcement content. An excessive amount of reinforcement powders weakens the interactions both among the particles themselves

and with the matrix alloy, thereby limiting the formation of a sound and well-bonded microstructure at the interface. The more gradual decrease observed at 150 °C, 175 °C, and 200 °C, despite the presence of the β phase, is due to the closure of pores between titanium powders under the effect of temperature, which minimizes structural defects. In contrast to yield strength and compressive strength, the best fracture strain values were obtained at 200 °C (figure 5(c), green line). In the composite samples, which exhibited behavior similar to conventional materials, the fact that higher fracture strain values were achieved even at the highest titanium content compared to the monolithic matrix alloy is attributed to the matching crystal structures of the matrix and reinforcement materials. The matching crystal structures of the matrix and reinforcement materials significantly contribute to the formation of a sound and well-bonded interface. High reinforcement content adversely affected the fracture strain as well, similar to its effect on yield and compressive strengths. This effect becomes more pronounced with increasing test temperatures (figure 5(c), lines other than the red one). Even at the highest titanium contents, the composite materials exhibited superior mechanical properties compared to the matrix alloy at both room and elevated temperatures. These samples, with their mechanical properties such as yield strength, compressive strength, and fracture strain, represent a significant alternative to many conventional materials used in industrial applications. In particular, for transportation applications in air, sea, and land vehicles, their good mechanical properties at both room and elevated temperatures, combined with low density, make them a compelling alternative to materials such as iron, steel, and aluminum.

4. Conclusions

The microstructural characteristics of titanium-reinforced magnesium matrix composites produced via hot-press sintering were investigated using FESEM, EDX, and XRD analyses. The yield strength, compressive strength, and fracture strain behaviors of the composite materials at room and elevated temperatures were revealed through mechanical tests conducted at various temperatures. The findings obtained from the morphological and mechanical tests are summarized below in a numbered list.

- It was determined that the theoretical and experimental densities of the monolithic alloy and composites were very similar, and the porosity in all samples was below 1%.
- Microstructural analyses revealed that titanium particles were located at the grain boundaries of the matrix alloy. Examinations identifying only the α-Mg, β-$Mg_{17}Al_{12}$, and Ti phases showed no evidence of porosity or the formation of any secondary phase at the interface between the two materials.
- Mechanical tests showed that the highest yield strength, compressive strength, and fracture strain values at both room and elevated temperatures were obtained in the sample containing 20 vol.% titanium.
- The addition of titanium not only resulted in significant increases in yield and compressive strengths but also led to notable improvements in fracture strain. Even at the maximum reinforcement content, higher fracture strain values were achieved compared to the monolithic alloy.
- The Ti_p/AZ91 samples stand out as a viable alternative to conventional materials in industrial applications such as automotive, due to their relatively good mechanical properties at both room and elevated temperatures, as well as their low density.

Acknowledgment

The author gratefully acknowledges the financial support of the Scientific Research Projects Coordination Unit at Van Yüzüncü Yıl University for this study (Project No: FBA-2024-11128).

Data availability statement

All the data required are available within the article.

Funding

This research was funded by the Scientific Research Projects Coordination Unit of Van Yüzüncü Yıl University, Turkey, under Grant Number FBA-2024-11128.

Conflict of interest

There is no conflict of interest.

Author contributions

The article is single-authored, and all contributions belong to the author.

ORCID iD

Fevzi Kelen 0000-0003-3900-4503

References

[1] Friedrich H and Schumann S 2001 Research for a "new age of magnesium" in the automotive industry *J. Mater. Process. Technol.* **117** 276–81
[2] Kelen F 2014 Motorlu taşıt emisyonlarının insan sağlığı ve çevre üzerine etkileri *Yüzüncü Yıl Üniversitesi Fen Bilimleri Enstitüsü Dergisi* **19** 80–87 (available at: https://izlik.org/JA42SJ58LD)
[3] Shahbeigi Roodposhti P, Sarkar A, Murty K l and Scattergood R O 2016 Effects of microstructure and processing methods on creep behavior of AZ91 magnesium alloy *J. Mater. Eng. Perform.* **25** 3697–709
[4] Kumar L G S, Thirumalaikumarasamy D, Karthikeyan K, Mathanbabu M, Ashokkumar M and Ramachandran C S 2023 An overview of recent trends and challenges of post treatments on magnesium alloys *Mater. Today Proc.* **78** 700–7
[5] Bharathi P and Sampath Kumar T 2023 Latest research and developments of ceramic reinforced magnesium matrix composites *a comprehensive Rev. Proc. Inst. Mech. Eng. E* **237** 1014–35
[6] Kumar T N, Kumar S V, Krishna V D S, Irfan S M and Kumar D S 2022 Particulate based AZ91 magnesium hybrid composites–a short review *Adv. Sci. Technol.* **120** 51–59
[7] Ho K F, Gupta M and Srivatsan T S 2004 The mechanical behavior of magnesium alloy AZ91 reinforced with fine copper particulates *Mater. Sci. Eng. A* **369** 302–8
[8] Hassan S F, Ho K F and Gupta M 2004 Increasing elastic modulus, strength and CTE of AZ91 by reinforcing pure magnesium with elemental copper *Mater. Lett.* **58** 2143–6
[9] Kelen F 2025 Assessing microstructural and mechanical characteristics of Ni/AZ91 composites manufactured using hot pressing technique for automotive applications *Mater. Chem. Phys.* **339** 130793
[10] Kelen F 2023 Nikel partiküller ile takviye edilmiş magnezyum matrisli kompozitlerin üretimi ve karakterizasyonu *Afyon Kocatepe Üniversitesi Fen Ve Mühendislik Bilimleri Dergisi* **23** 1318–27
[11] Tang B, Li J B, Ye J L, Luo H, Wang Y T, Guan B and Pan F S 2022 Strengthening mechanism and microstructure of deformable Ti particles reinforced AZ91 composite *Acta Metall. Sin.* **35** 1935–45
[12] Luo H, Li J, Wang Y, Ye J, Zhang Z, Guan B, Chen X, Zheng K and Pan F 2023 Influence of Ti particle sizes on microstructure and mechanical behaviors of AZ91-Ti composites under different loading paths *Mater. Sci. Eng. A* **886** 145723
[13] Chen X, Li J, Wang Y, Luo H, Guan B, Chen X and Pan F 2023 Hot deformation behaviors of titanium particles reinforced AZ91 composite *J. Mater. Res. Technol.* **24** 200–14
[14] Pu D, Wu S, Yang H, Chen X, Li J, Feng X and Pan F 2023 Effect of Ti particles on microstructure and mechanical properties of TiP/AZ91 composites *J. Mater. Res. Technol.* **22** 1362–74
[15] Jiao J, Gu Y, Zhang J, Lian Y, Li X, Zheng K and Pan F 2025 The growth behavior and performance of microarc oxidation coating on AZ91/Ti composite: influence of Ti-reinforcement phase and electrolyte *J. Magnes. Alloys* **13** 1160–75
[16] Kumar N, Bharti A and Chauhan A K 2021 Effect of Ti reinforcement on the wear behaviour of AZ91/Ti composites fabricated by powder metallurgy *Mater. Phys. Mech.* **47** 600–7
[17] Kumar N, Bharti A and Saxena K K 2021 Effect of Ti reinforcement on the physical and mechanical properties of AZ91/Ti composites *Indian J. Eng. Mater. Sci.* **28** 602–7
[18] Wu B, Li J, Ye J, Tan J, Liu L, Song J and Pan F 2021 Work hardening behavior of Ti particle reinforced AZ91 composite prepared by spark plasma sintering *Vacuum* **183** 109833
[19] Xiao L, Liu T T, Chu Y, Song B, Zhao J, Chen X H and Pan F S 2024 Effect of Ti particles on the microstructure and mechanical properties of AZ91 magnesium matrix composites *Acta Metall. Sin.* **37** 513–24
[20] Luo H, Li J, Ye J, Wang Y, Chen X, Zheng K and Pan F 2024 Enhancing the mechanical properties and thermal conductivity of Ti/AZ91 composites through integrated extrusion and rolling continuous deformation processing *J. Alloys Compd.* **1002175506**
[21] Yang H, Cui J, Zhou Y, Tan J, Chen X, Huang G and Pan F 2023 Microstructures and the improved mechanical properties of AZ91 alloy by incorporating Ti-6Al-4V particles *J. Mater. Res. Technol.* **26** 7340–53
[22] Luo H, Li J, Ye J, Lu Y, Tan J, Song J and Pan F 2022 Influence of Ti-6Al-4V particles on the interfacial microstructure and strength-ductility synergetic mechanism of AZ91 magnesium alloy *Mater. Charact.* **191** 112154
[23] Kelen F, Gavgali M and Aydogmus T 2018 Microstructure and mechanical properties of a novel TiNi particulate reinforced AZ91 metal matrix composite *Mater. Lett.* **233** 12–15

[24] Kelen F, Gavgali M and Aydoğmuş T 2025 TiNi Particle-Reinforced Magnesium Matrix Composites: production, Microstructure, Phase Transformations, and Mechanical Properties *Adv. Eng. Mater.* **27** 2402277
[25] Aydogmus T 2015 Processing of interpenetrating Mg–TiNi composites by spark plasma sintering *Mater. Sci. Eng. A* **624** 261–70
[26] Kelen F 2023 Novel magnesium matrix hybrid composites manufactured through powder metallurgy technique *Mater. Today Commun.* **35** 106348
[27] Kelen F 2023 Fabrication, microstructure and mechanical properties of novel titanium and nickel micro-particulates reinforced AZ91D magnesium alloy metal matrix hybrid composites *J. Alloys Compd.* **968** 171999
[28] Veiga C, Davim J P and Loureiro A J R 2012 Properties and applications of titanium alloys: a brief review *Rev. Adv. Mater. Sci.* **32** 133–48
[29] Welsch G, Boyer R and Collings E W 1993 *Materials Properties Handbook: Titanium Alloys* (ASM International)
[30] Aruna M, Nagabhooshanam N, Parihar P S, Kedia N, Satya G, Maranan R and Sathiyamurthy S 2026 Titanium dioxide/alumina nanoparticles on microstructural and mechanical properties of AZ61 alloy composites *J. Mech. Sci. Technol.* **40** 1059–64
[31] Guo W, Shi J, Lü S, Xiang K, Yan Z, Wu Z and Zhang X 2026 Effects of Ti particle on the microstructural evolution and mechanical properties of TiP/AZ61 composites: experimental studies and first-principles calculations *J. Alloys Compd.* **186266**
[32] Hassan S F and Gupta M 2002 Development of ductile magnesium composite materials using titanium as reinforcement *J. Alloys Compd.* **345** 246–51
[33] Umeda J, Kawakami M, Kondoh K, Ayman E S and Imai H 2010 Microstructural and mechanical properties of titanium particulate reinforced magnesium composite materials *Mater. Chem. Phys.* **123** 649–57
[34] Perez P, Garces G and Adeva P 2004 Mechanical properties of a Mg–10 (vol.%) Ti composite *Compos. Sci. Technol.* **64** 145–51
[35] Pc E, Radhakrishnan G and Emarose S 2021 Investigation into physical, microstructural and mechanical behaviour of titanium dioxide nanoparticulate reinforced magnesium composite *Mater. Technol.* **36** 575–84
[36] Ye J, Chen X, Luo H, Zhao J, Li J, Tan J and Pan F 2022 Microstructure, mechanical properties and wear resistance of Ti particles reinforced AZ31 magnesium matrix composites *J. Magnes. Alloys* **10** 2266–79
[37] Dinaharan I, Zhang S, Chen G and Shi Q 2020 Titanium particulate reinforced AZ31 magnesium matrix composites with improved ductility prepared using friction stir processing *Mater. Sci. Eng. A* **772** 138793
[38] Gao P, Han S, Zhang Y, Fang B, Zhang X, Wang X, Ding H, Zheng K and Pan F 2024 Investigation on the interface bonding and reinforcement mechanism of nano Ti/AZ31 magnesium matrix composites *J. Mater. Res. Technol.* **30** 4908–19
[39] Kim S, Kim G, Lee W, Lee H S and Jeung W 2017 A novel method to fabricate reinforced Ti composites by infiltration of Al (Mg) into porous titanium *J. Alloys Compd.* **715** 404–12
[40] Pu D, Chen X, Wang J, Tan J, Li J, Yang H and Pan F 2023 Effect of Ti particles on the microstructure and mechanical properties of as-extruded Titanium-reinforced Mg-9Gd-4Y–1Zn–1Mn matrix composites *Mater. Sci. Eng. A* **879** 145278
[41] Murray J L 1982 The Al— Mg (aluminum— magnesium) system *J. Phase Equilib.* **3** 60–74
[42] Mohazzab P 2017 Archimedes' principle revisited *J. Appl. Math. Phys.* **5** 836–43
[43] Kumar A, Kumar S, Mukhopadhyay N K, Yadav A and Winczek J 2020 Effect of SiC reinforcement and its variation on the mechanical characteristics of AZ91 composites *Materials* **13** 4913
[44] Pekguleryuz M O and Kaya A A 2003 Creep resistant magnesium alloys for powertrain applications *Adv. Eng. Mater.* **5** 866–78
[45] Alam T and Ansari A H 2017 Review on Aluminium and Its Alloys for automotive applications *Int. J. Adv. Technol. Eng. Sci.* **5** 278–94
[46] Yang H, Chen X, Huang G, Song J, She J, Tan J and Pan F 2022 Microstructures and mechanical properties of titanium-reinforced magnesium matrix composites: review and perspective *J. Magnes. Alloys* **10** 2311–33
[47] Yang H, Liu S, Xu J, Jiang B, Wu L, Yang H and Zheng K 2026 Effects of nano-Ti particles on the microstructure, mechanical properties, and corrosion properties of Mg-Gd-Y-Zn-Zr alloy *J. Alloys Compd.* **186254**
[48] Lütjering G E R D 1998 Influence of processing on microstructure and mechanical properties of ($\alpha+\beta$) titanium alloys *Mater. Sci. Eng. A* **243** 32–45
[49] Murray J L 1986 The Mg— Ti (magnesium-titanium) system *Bull. Alloy Phase Diagr.* **7** 245–8
[50] Raghavan V 2005 Al-Ti (aluminum-titanium) *J. Phase Equilib. Diffus.* **26** 171
[51] Okamoto H 2008 Ti-Zn (titanium-zinc) *J. Phase Equilib. Diffus.* **29** 211–2
[52] Zhao H, Shen J, Hu S, Chen Y, Sui Y and Hu N 2026 Effect of rotational speed on microstructure and mechanical properties of TC4 particle-reinforced magnesium matrix composites by WAAM-FSP technology *J. Alloys Compd.* **186032**
[53] Jang J E, Park B H, Younj H J, Cheng W L, Joo S H and Park S H 2026 Effect of Zn addition to Mg melt on microstructural characteristics of Mg–Ti composites fabricated via liquid metal dealloying *J. Magnes. Alloys* **102014**
[54] ASTME9-89a 2000 *Test Methods of Compression Testing of Metallic Materials at Room Temperature* (ASTM International)
[55] Hu H, Yu A, Li N and Allison J E 2003 Potential magnesium alloys for high temperature die cast automotive applications: a review *Mater. Manuf. Process.* **18** 687–717
[56] Saleh B, Jiang J, Fathi R, Xu Q, Wang L and Ma A 2020 Study of the microstructure and mechanical characteristics of AZ91–SiCp composites fabricated by stir casting *Arch. Civ. Mech. Eng.* **20** 71
[57] Sui X, Xu H, Jiang B, Wang Y, Hu M and Ji Z 2024 Effect of the TiB_2 content on the mechanical and tribological properties of TiB2/AZ91 composites fabricated by vacuum hot-press sintering process incorporating vacuum ball milling *Mater. Today Commun.* **40** 109722
[58] Sun Y, Zhang B, Yang C, Zhang Z, Liang T, Li T and Cai R 2022 Microstructure and mechanical properties of caliber rolled AlN/AZ91 composite *Mater. Sci. Eng. A* 853143779
[59] Kumar D and Thakur L 2023 Investigation on mechanical and wear performance of ultrasonic-assisted stir cast AZ91D/Al_2O_3 magnesium matrix composites *Met. Mater. Int.* **29** 2767–81